

EARTH PRESSURES UNDER GENERAL WALL MOVEMENTS

Y.S. Fang¹, F.P. Cheng¹, R.T. Chen²,
and C.C. Fan²

SYNOPSIS

In this paper, the finite element method is used to investigate the variation of horizontal earth pressure behind a rigid retaining wall for two categories of wall movements: (1) rotation about a point below its base (RBT mode); and (2) rotation about a point above its top (RTT mode). Triaxial tests and direct shear tests have been conducted to determine the hyperbolic parameters employed in the analyses. Numerical findings are compared with experimental results and traditional theories, and good agreements have been achieved. It is found that the mode of wall movement has a significant effect on the generation of earth pressure. For a wall under translational movement (T mode), the intensity and distribution of active earth pressure are in good agreement with Coulomb's solution. The RT (rotation about top), RB (rotation about base) and T modes are the three limiting movement modes that could occur to a rigid wall.

INTRODUCTION

When designing a gravity retaining wall, an engineer needs to know the intensity and distribution of lateral earth pressure acting against the relatively rigid structure. For design purposes, the classic Coulomb and Rankine theories, which assume a linear distribution of lateral earth pressure with depth, have been commonly adopted to evaluate the overall adequacy of the wall.

The lateral earth pressures induced by different wall movement modes have been studied with numerical methods by different researchers (Clough and Duncan 1971; Simpson and Wroth 1972; Nakai 1985; Potts and Fourie 1986). Their findings indicate that the distribution of earth pressure is highly dependent on the assumed mode of deformation. Experimental work investigating the variation of lateral earth pressure as a function of wall movement was first carried out by Terzaghi (1934). Sherif et al. (1984); Fang and Ishibashi (1986) reported experimental earth pressure distribution behind a rigid wall for three different wall movement modes: (1) rotation about the top (RT mode); (2) rotation about the base (RB mode); and (3) translation

¹ Associate Professor, Department of Civil Engineering, National Chiao Tung University, Hsinchu, Taiwan, 300, ROC.

² Formerly Graduate Student, Department of Civil Engineering, National Chiao Tung University, Hsinchu, Taiwan, 300, ROC.

(T mode). However, all of the investigations mentioned above were limited to a few specific types of wall displacements, which can not represent the general movement of the wall. It should be noted that, besides many other factors, the movement of a real retaining wall is dependent on the wall rigidity, construction method and support conditions provided.

As shown in Fig. 1, the general movements of a rigid retaining wall, moving away from the backfill, can be inducted into the following two categories:

- (1) rotation about a point below wall base, which simulate the sliding and overturning behavior of the wall. It is clear from Fig. 1 (a) that when n equals zero, this becomes the RB mode. On the other hand, as n approaches infinity, this becomes the T mode condition. As a result, this type of wall movement is abbreviated to RBT mode. However, it would be interesting to know if the earth pressure induced by the RBT mode, when n approaches a very large number, will be the same as that induced by the T mode.
- (2) rotation about a point above wall top, which simulates the behavior of a bridge abutment. The soil near the top of the wall is restrained laterally by the bridge deck, thus not allowed to move outward to mobilize full resistance within the soil. Meanwhile, the soil at a lower elevation exerts a drag type of shear force upon the overlying soil. It may be seen that when n equals zero, this becomes the RT mode. Therefore, this category of wall movement is termed RTT mode as illustrated in Fig. 1 (b).

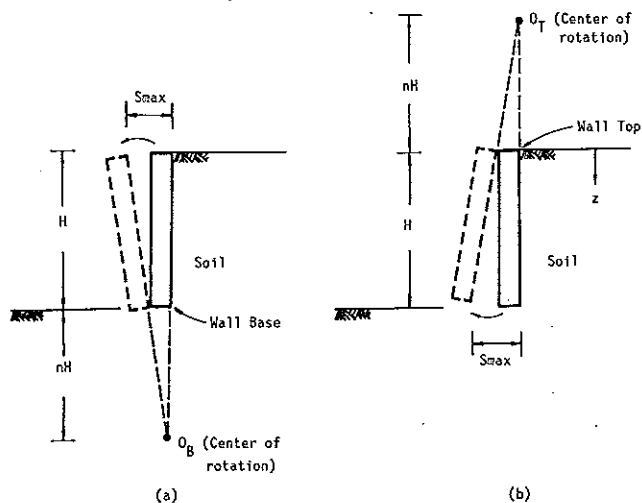


Fig. 1 General Wall Movements of Rigid Wall:
 (a) Rotation about a Point below Wall Base (RBT Mode);
 (b) Rotation about a Point above Wall Top (RTT Mode)

In this paper, the finite element method is used to study the variation of earth pressure induced by various movements of a rigid wall. The well-accepted hyperbolic stress-strain relationship (Duncan and Chang, 1970; Clough and Duncan, 1971) is chosen to model the backfill and soil-structure interaction. Triaxial tests and direct shear tests have been conducted on Ottawa sand to obtain realistic parameters. Hyperbolic parameters thus determined have been assigned to a newly developed plane-strain finite element program, named SOILPR, to calculate the variation of horizontal soil stresses against the wall as a function of wall movement. To validate the effectiveness of the analyses, numerical findings are compared with published experimental results and traditional earth pressure theories. The present study discusses the change of stresses acting on the wall from the at-rest state to the active state only.

BACKFILL BEHAVIOR

Stress-strain Relationships

The hyperbolic stress-strain relationships were developed by Duncan and Chang (1970) for incremental analyses of soil deformations, where nonlinear behavior is modeled by a series of linear increments. For plane strain conditions, Duncan (1980) suggested that the stress-strain relationship may be expressed in terms of Young's modulus and bulk modulus as follow:

$$\begin{Bmatrix} \Delta\sigma_x \\ \Delta\sigma_y \\ \Delta\tau_{xy} \end{Bmatrix} = \frac{3B}{9B-E} \begin{bmatrix} (3B+E) & (3B-E) & 0 \\ (3B-E) & (3B+E) & 0 \\ 0 & 0 & E \end{bmatrix} \begin{Bmatrix} \Delta\epsilon_x \\ \Delta\epsilon_y \\ \Delta\gamma_{xy} \end{Bmatrix} \quad (1)$$

in which $\Delta\sigma_x$, $\Delta\sigma_y$ and $\Delta\tau_{xy}$ are stress increments; $\Delta\epsilon_x$, $\Delta\epsilon_y$, and $\Delta\gamma_{xy}$ are strain increments; B is bulk modulus; and E is Young's modulus. Both B and E vary with confining pressure. The procedures used to approximate these characteristics are briefly summarized in the subsequent paragraphs.

Empirical Equations

Kondner (1963) proposed that the stress-strain curves for a number of soils may be represented by the hyperbolic equation:

$$(\sigma_1 - \sigma_3) = \frac{\epsilon}{\frac{1}{E_i} + \frac{R_f \epsilon}{(\sigma_1 - \sigma_3)_f}} \quad (2)$$

in which E_i = initial tangent modulus; R_f = failure ratio; ϵ = normal strain; σ_1 and σ_3 = major and minor principal stresses; and $(\sigma_1 - \sigma_3)_f$ = stress difference

at failure, which can be determined by using the Mohr-Coulomb strength equation. The variation of E_t with confining pressure, σ_3 , is represented by the following equation suggested by Janbu (1963):

$$E_t = K P_a \left(\frac{\sigma_3}{P_a} \right)^{n_1} \quad (3)$$

The parameter K in equation (3) is the modulus number; n_1 is the modulus exponent, and P_a is the atmospheric pressure.

Duncan and Chang (1970) stated that the stress-strain relationship expressed by equation (2) may be used in incremental stress analyses, since it is possible to determine the value of the tangent modulus corresponding to any point on the stress-strain curve. By differentiating equation (2) with respect to ϵ , the following equation can be derived:

$$E_t = \left[1 - \frac{R_f (1 - \sin \phi) (\sigma_1 - \sigma_3)}{2c \cos \phi + 2\sigma_3 \sin \phi} \right]^2 K P_a \left(\frac{\sigma_3}{P_a} \right)^{n_1} \quad (4)$$

in which E_t = tangent modulus; and c and ϕ = the Mohr-Coulomb strength parameters. The increase of bulk modulus with increasing confining pressure can be approximated by the following empirical equation:

$$B = K_b P_a \left(\frac{\sigma_3}{P_a} \right)^m \quad (5)$$

in which K_b = bulk modulus number; and m = bulk modulus exponent. By varying the values of tangent modulus and bulk modulus as stresses vary within the soil, it is possible to employ equation (1) to model the nonlinear stress-dependent behavior of the backfill.

In order to establish a realistic stress-strain relationship of the backfill, triaxial tests simulating lateral expansion behavior of the backfill have been conducted. Air-dried Ottawa sand (ASTM C-109, $D_{10} = 0.17$ mm, $D_{30} = 0.22$ mm, $D_{50} = 0.28$ mm, $D_{60} = 0.31$ mm, $G_s = 2.65$, $e_{max} = 0.71$ and $e_{min} = 0.49$) is used in the experiments during this investigation. Typical test results are listed in Table 1. Detailed procedures to estimate the parameter values follow Duncan et al. (1980). Since the hyperbolic model can not successfully simulate the post-peak behavior for dense sand, all tests are conducted on loose sand with a relative density of 34 percent. As a result, the scope of this study is limited to uncompacted cohesionless backfill only.

INTERFACE BEHAVIOR

Empirical Equations

Clough and Duncan (1971) suggested that the nonlinear stress-dependent inter-

Table 1 Summary of Hyperbolic Parameters.

Backfill	Parameter	Symbol	Value
Backfill	Unit weight, in kN/cu m	γ	15.6
	Angle of internal friction, in degrees	ϕ	33.5
	Coefficient of earth pressure at-rest ($K_o = 1 - \sin \phi$)	K_o	0.448
	Cohesion intercept, in kN/sq m	c	0
Loose sand backfill	Primary loading modulus number	K	623
	Modulus exponent	n_1	0.773
	Failure ratio	R_f	0.95
	Bulk modulus number	K_b	236
	Bulk modulus exponent	m	0.55
Wall-backfill and base-backfill interfaces	Friction angle, in degrees	δ	32.2
	Stiffness number	K_1	74,100
	Stiffness exponent	n_2	0.79
	Failure ratio	R_f	0.90

face behavior, which acts between the backfill and the wall, may be approximated by the following hyperbolic relationship:

$$\tau = \frac{\Delta_s}{\frac{1}{K_{si}} + \frac{R_f}{\tau_f} \Delta_s} \quad (6)$$

in which τ = interface shear stress; Δ_s = interface shear displacement; K_{si} = initial tangent shear stiffness; R_f = failure ratio; and τ_f = shear stress at failure. Both the initial tangent shear stiffness and the shear strength depend on the value of normal stress, σ_n , on the interface. The shear strength of interface may be expressed in terms of the wall friction angle δ ($\tau_f = \sigma_n \tan \delta$), and K_{si} may be expressed using the equation suggested by Janbu (1963):

$$K_{si} = K_1 \gamma_w \left(\frac{\sigma_n}{P_a} \right)^{n_2} \quad (7)$$

in which K_1 = stiffness number; n_2 = stiffness exponent; γ_w = unit weight of water. By using equations (6) and (7), the nonlinear, stress dependent behavior of interface may be expressed in terms of the four parameters K_1 , n_2 , R_f and δ . A convenient method to approximate nonlinear interface behavior is to perform incremental

analyses, by changing the soil properties for each stage of the analysis. The tangent stiffness value, K_{st} , may be derived by differentiate equation (6) with respect to Δ_s .

$$K_{st} = K_1 \gamma_w \left(\frac{\sigma_n}{P_s} \right)^{n_2} \left(1 - \frac{R_f \tau}{\sigma_n \tan \delta} \right)^2 \quad (8)$$

Clough and Duncan (1971) concluded that the tangent stiffness value based upon these stress values has been found to provide a good approximation for the interface behavior, provided that the increments employed were sufficiently small.

Interface Elements

Four noded one-dimensional interface elements developed by Goodman *et al.* (1968) are arranged along the soil-wall interface to simulate the interface interaction. The properties of the interface element consist of a normal stiffness, K_n , and a shear stiffness, K_s , which are related to the normal and shear stresses acting on the element as follows:

$$K_n \Delta_n = \sigma_n \quad (9)$$

$$K_s \Delta_s = \tau \quad (10)$$

in which Δ_n = average relative normal displacement across the element; and Δ_s = average relative shear displacement along the element. The value of K_s was calculated using equation (8). To prevent significant overlap of the adjacent elements, K_n was made to be very high ($K_n = 10^8$ kN/m³). If a gap opens between the wall and the backfill, both K_s and K_n were assigned very small values. For greater detail regarding the interface element, the reader is referred to Goodman *et al.* (1968).

Potyondy (1961) studied the interface behavior between various soils and construction materials by performing direct shear tests. In a similar way, direct shear tests have been conducted for this investigation, to establish a valid relationship between the backfill and the wall. The construction material, such as a 60 mm by 60 mm concrete block specimen, is placed into the lower shear box while the cohesionless backfill is gently poured into the upper shear box. The stress-displacement data are measured from the proving ring and dial gage during the shearing process. Wall friction angle and hyperbolic parameters estimated from laboratory experiments, following Clough and Duncan's recommendations are also listed in Table 1. All analyses in this paper deal with the earth pressure acting between the backfill and rough concrete, which is commonly used to construct a gravity wall.

NUMERICAL MODELING

The finite element mesh used for this study is shown in Fig. 2. Eight noded quadratic isoparametric elements are employed to model the soil behavior under

EARTH PRESSURES UNDER WALL

plane strain condition. Four noded one-dimensional interface elements are arranged along the soil-wall interface to simulate the interface characteristics. Boundary conditions assumed for the problem are also illustrated in Fig. 2. To compare with experimental results, a 1.0 m high wall is modeled. Due to the existence of the interface elements, slippage between the soil and wall is permitted. Beginning from an at-rest pressure condition, the wall was moved away from the backfill in a series of increments, until an active earth pressure condition was reached. Initial stresses of $\sigma_v' = \gamma \cdot z$ and $\sigma_h' = K_0 \sigma_v'$ are assumed to act in the backfill prior to loading. K_0 values are calculated following the Jaky's equation ($K_0 = 1 - \sin \phi$). It should be mentioned that, due to the wall construction sequence, the initial stress condition in the field would be much more complicated than the ideal condition assumed.

In order to discuss the influence of wall movement modes, earth pressures induced by the two major categories of displacements are presented in the subsequent sections.

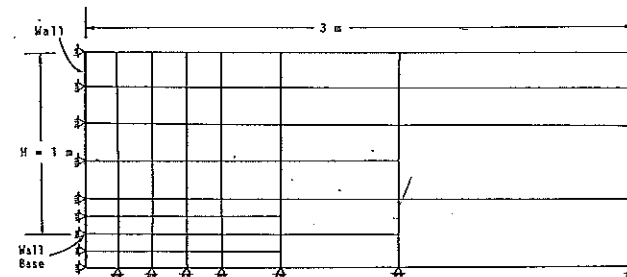


Fig. 2 Finite Element Mesh

PRESSURE DISTRIBUTION

Translational Wall Movement (T Mode)

As discussed in the introductory part of this article, the general movements of a rigid wall can be divided into the RBT mode and the RTT mode. However, for either case, as the center of rotation moves vertically to infinity, the movement actually becomes the translational mode. In this regard, for comparison purposes, it would be beneficial to investigate the lateral stresses induced by T mode as a start.

The distributions of horizontal earth pressure, σ_h , induced by a rough concrete wall moving away from the backfill under T mode are shown in Fig. 3. From the figure it can be seen that the lateral stresses acting near the base of the wall decrease somewhat faster than that at a higher elevation. The intensity and distribution of active earth pressure is in good agreement with the values calculated from

Coulomb's theory. Since the wall movement under T mode satisfies one of Coulomb's assumptions: the wall moves sufficiently to develop a state of plastic equilibrium in the backfill. Therefore, it would be reasonable to expect that the total active thrust and its point of application could be predicted by Coulomb's theory.

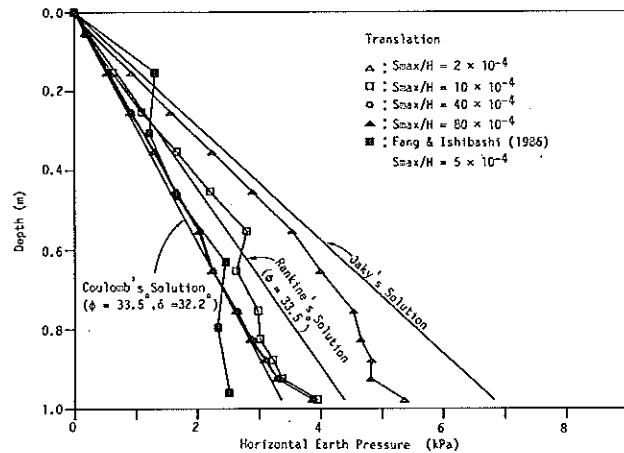


Fig. 3 Distributions of Horizontal Earth Pressure at Different Translational Wall Displacements

Fang and Ishibashi (1986) conducted experiments on a model retaining wall system. The instrumented center wall is 1.02 m wide and 1.04 m high. Air-dried loose Ottawa sand ($\phi = 34^\circ$, $\delta = 20^\circ$, and $D_r = 28\%$) was used as backfill in the model test. The experimental active earth pressure distribution behind the model wall under T mode is also displayed in Fig. 3. From these data, it is clear that both analytical and experimental results are in reasonably good agreement with Coulomb's solution. However, due to the asymptotic characteristics of the hyperbolic model, greater wall movement is required in the analytical calculation to reach its active state. From the same figure, it is seen that Rankine's solution, which does not take the effect of wall friction into consideration, overestimates the active earth pressure induced by T mode.

Wall Rotation about a Point below Its Base (RBT Mode)

The horizontal earth pressure behind a wall moving away from the backfill under RBT mode is discussed in this section. As indicated in Fig. 1 (a), with the change of O_B position in the vertical direction, infinite sets of wall movement could exist. However, only representative n values of 0.00, 0.05, 0.10, 0.20, 0.50, 1.0, 2.0 and 5.0 are studied in this paper.

Fig. 4 shows the analytical results as a function of normalized wall movement for the n equals zero condition. It is clear from the figure that the horizontal stresses calculated at upper elevations decrease very quickly. However, the earth pressures near the base decrease slowly with the wall rotation. This is because the backfill near the base can not expand sufficiently in the horizontal direction under the designated wall movement. Stress concentration is observed near the lower boundary of the wall. This behavior has also been reported by Potts and Fourie (1986), and Nakai (1985). Experimental stress distribution plotted in Fig. 4 justifies that Coulomb's theory can be used to estimate the active stress acting at upper elevations of the wall under RB mode. Measured active pressures acting near the base of the wall are indeed greater than Coulomb's and Rankine's predictions.

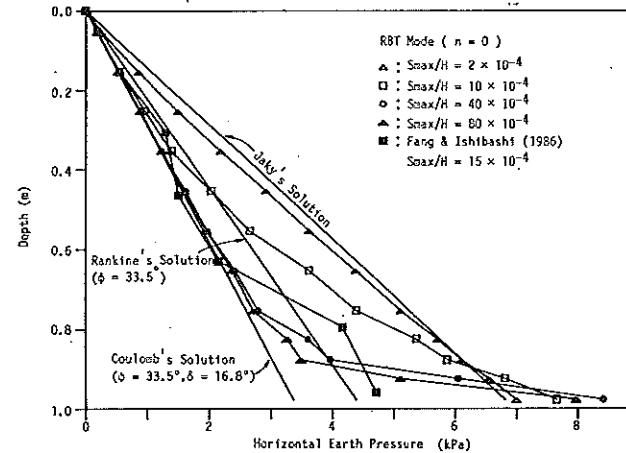


Fig. 4 Distributions of Horizontal Earth Pressure at Different Wall Movements (RBT Mode, $n = 0$)

For the RBT category of wall movement, it is reasonable to expect that different n values would result in different patterns of wall displacements and different earth pressure distributions. Fig. 5 shows the change of pressure distribution under RBT mode for n equals 0.05. In this figure, stress concentration is also observed near the base. However, in comparison with the curves for n equals zero, much of the extra stress has been relaxed due to the small amount of lateral expansion of backfill near the base of the wall.

Variation of horizontal stress distribution for n equals 0.50 is illustrated in Fig. 6. It is clear from the figure that lateral stresses acting on the upper 95 percent of the wall are in good agreement with Coulomb's theory. In comparison with Fig. 5, it may be seen that the high stress acting near the base decrease rapidly with the slight increase of n value. Analytical results indicate that further increase of n result in practically identical active pressure distribution. It is interesting to compare Fig. 6

with Fig. 3. From these data, it is clear that for n equals 0.50, the active earth pressure distribution induced by the RBT mode is nearly the same as that induced by T mode. The physical meaning of this finding is that, unless the base of the wall is firmly fixed in the horizontal direction, the active earth pressure exerted on the back of the wall can be adequately predicted using the Coulomb's theory.

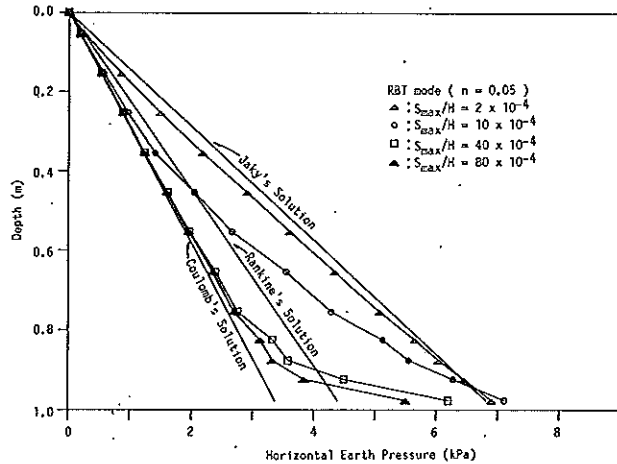


Fig. 5 Distributions of Horizontal Earth Pressure at Different Wall Movements (RBT Mode, $n = 0.05$)

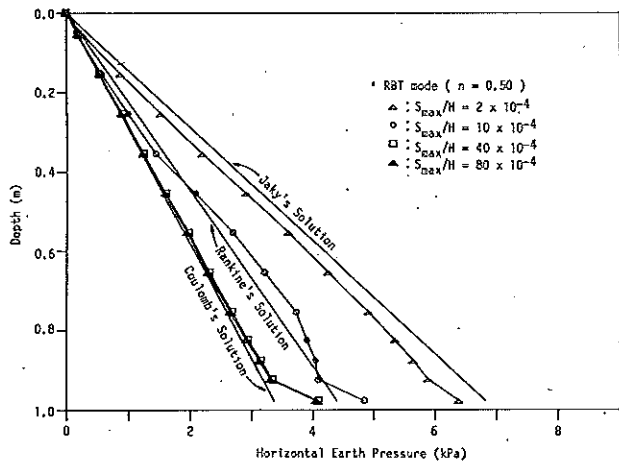


Fig. 6 Distributions of Horizontal Earth Pressure at Different Wall Movements (RBT Mode, $n = 0.50$)

Wall Rotation about a Point above Its Top (RTT Model)

The horizontal earth pressure behind a retaining wall under RTT mode is discussed in this section. The variation of earth pressure distribution for RT mode is illustrated in Fig. 7. It is clear that the stress near the base decreases rapidly with increasing wall displacement, and finally a value consistent with Coulomb's solution is reached. On the other hand, stress concentration is clearly demonstrated near the top of the wall. The build up of lateral stresses due to soil arching was first introduced by Terzaghi (1943). The experimental curve obtained by Fang and Ishibashi (1986) validates the existence of the arching stress, although the calculated peak arching stress is greater than the test value. It is clear from the experimental curve that the actual stress intensity at a lower elevation is smaller than that obtained from FEM analysis. The discrepancy is probably due to the fact that soils near the base tend to flow outward to fill the space generated by the wall rotation, and the hyperbolic model used is unable to model this specific soil behavior. For design considerations, if the wall is restrained laterally near the top while its lower portion is allowed to move, the earth pressure developed will not follow Coulomb's theory.

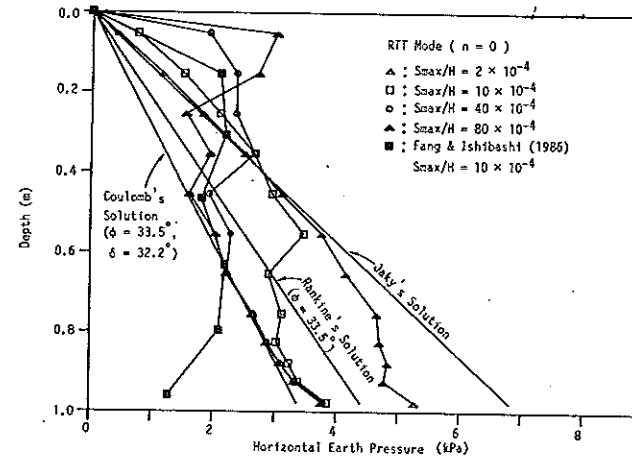


Fig. 7 Distributions of Horizontal Earth Pressure at Different Wall Movements (RTT Mode, $n = 0$)

Fig. 8 shows the variation of lateral pressure for n equals 0.20. It is evident from the figure that the intensity of arching stress decreases with increasing n value. The distribution of σ_h behind a wall under RTT mode for n equals 2.0 is indicated in Fig. 9. From simple geometry, a greater n value implies more lateral expansion allowed for the backfill near the top. It may be seen from Fig. 9 that both the horizontal pressure near the top and that near the base decrease with increasing wall movement, until an active earth pressure in good agreement with Coulomb's solution has been reached. Further analytical studies indicate that the arching effect could be

neglected for n values greater than 2.0. It is significant to compare Fig. 9 with Fig. 3 and Fig. 6. From these figures it may be concluded that for n exceeds a limiting value (0.50 for RBT mode and 2.0 for RTT mode), the active earth pressure exerted on the back of the wall could be estimated by Coulomb's theory.

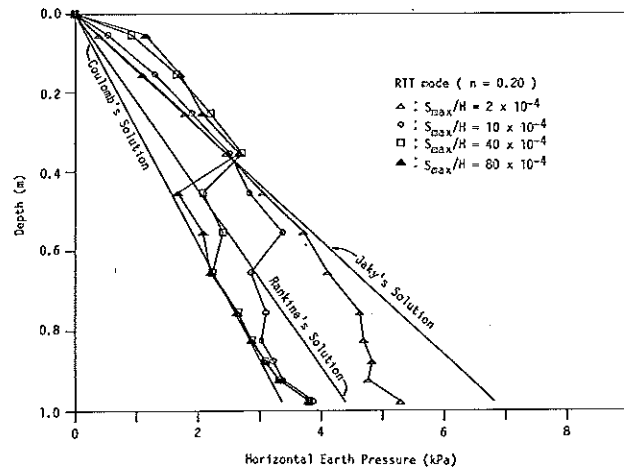


Fig. 8 Distributions of Horizontal Earth Pressure at Different Wall Movements (RTT Mode, $n = 0.20$)

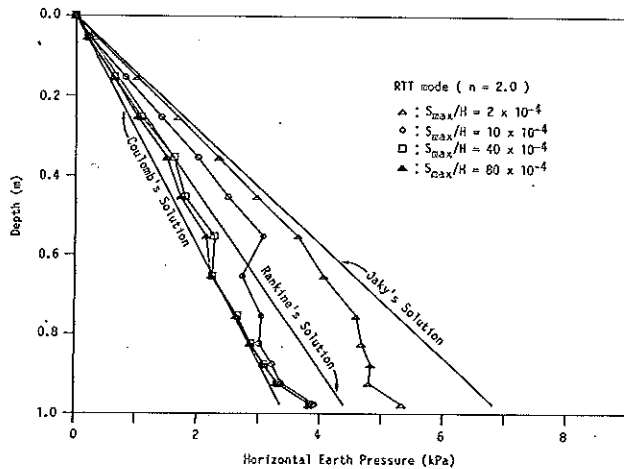


Fig. 9 Distributions of Horizontal Earth Pressure at Different Wall Movements (RTT Mode, $n = 2.0$)

TOTAL THRUST AND ITS POINT OF APPLICATION

For engineering purposes, in evaluating the adequacy of a gravity-type retaining wall, it is often necessary to determine its factor of safety against sliding and overturning. As a result, the magnitude and the point of application of the total thrust is of critical importance to the design engineer. The horizontal total thrust P_h , which is illustrated schematically in Fig. 10, is the summation of lateral earth pressures per unit length of wall.

Total Thrust

Fig. 10 shows the analytical horizontal earth pressure coefficient, K_h , as a function of normalized wall movement, under RBT mode for n values ranging from 0.00 to 5.00. It is evident from the figure that the magnitude of P_h decreases with the outward movement of the wall. Finally, a limiting value of K_h is reached, and this value is defined as the active earth pressure coefficient $K_{A,h}$. As emphasized in the preceding section, the intensity of the concentrated stress acting near the base dissipates with increasing n values. As a result, the magnitude of P_h decreases with increasing n value. It is clear from Fig. 10 that the curve for $n = 5.0$ is practically the same as that induced by T mode, which constitutes the lower bound for this family of curves. Due to the existence of extra stress near the base, all the calculated $K_{A,h}$ values are higher than Coulomb's solution for $\phi = 32.2^\circ$. For comparison purposes, the total thrust for wall friction angle $\delta = \phi/2 = 16.8^\circ$ which is commonly used by the design engineer is also plotted in Fig. 10. Rankine's solution obviously overestimates the magnitude of the active total thrust.

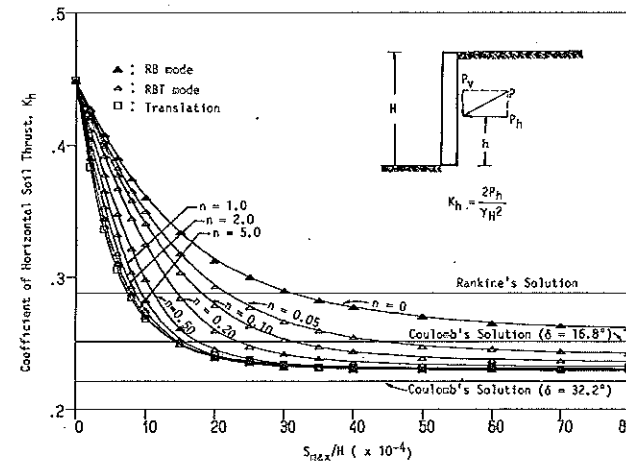


Fig. 10 Horizontal Earth Pressure Coefficient K_h versus wall Movement (RTT Mode)

The variation of K_h as a function of wall movement under RTT mode is shown in Fig. 11. It is clear from the figure that, before achieving an active state, the magnitude of P_h decreases with increasing wall displacement. Due to the exertion of the arching stress, the horizontal active thrust $P_{A,h}$ is greater than Coulomb's solution. As a sequence of the dissipation of arching stress, the magnitude of $K_{A,h}$ decreases with increasing n value. It is evident from Fig. 11 that the upper bound and the lower bound for this family of curves are represented by the RT mode (n equals zero) and T mode (n approaches infinity), respectively.

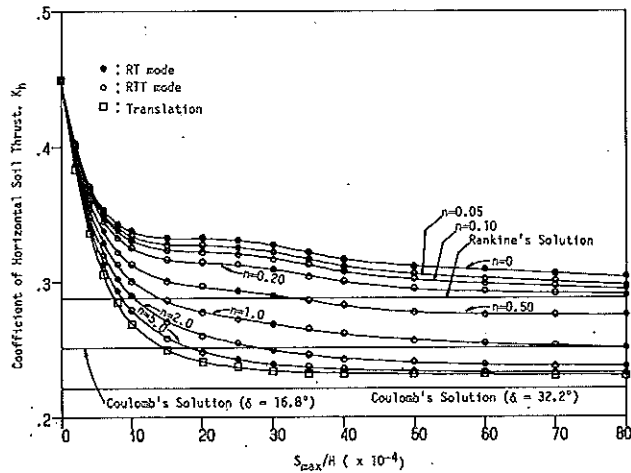


Fig. 11 Horizontal Earth Pressure Coefficient K_h versus wall Movement (RTT Mode)

Experimental variation of K_h as a function of wall movement for RB, RT and T modes (Fang, 1983) are indicated in Fig. 12. The at-rest earth pressures employed in the analysis are calculated following Jaky's formula. The experimental at-rest earth pressures are higher due to the effect of backfill compaction, as reported by Sherif et al. (1984), and Duncan and Seed (1986). It is seen from Fig. 10 and 12 that the analytical K_h versus s_{max}/H relationship for RB mode is in fairly good agreement with the test value. The horizontal active earth pressure coefficient obtained from both methods are 0.25. It is clear from Fig. 10, 11 and 12 that the $K_{A,h}$ value can be estimated by the finite element method with reasonable accuracy. The K_h versus s_{max}/H relationship for the translational mode constitutes the lower bound for both the RBT and RTT type of wall movements. Therefore, if a special type of wall motion occurs, the Coulomb's theory, which assumes that the entire wall moves sufficiently, tends to underestimate the total thrust acting on the wall.

EARTH PRESSURES UNDER WALL

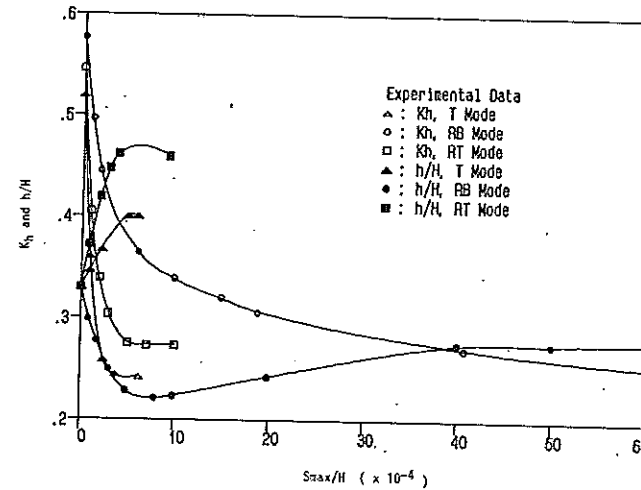


Fig. 12 Experimental Horizontal Earth Pressure Coefficient K_h , Relative Height of Resultant Pressure h/H , versus Wall Movement (data after Fang, 1983)

Point of Application

The variation of point of application of the total thrust as a function of wall movement for both RBT and RTT modes are shown in Fig. 13. From these data it may be seen that, under the RB mode, due to the rapid drop of earth pressure at upper elevations (see Fig. 4), the acting point of P_h is lowered when the wall starts to

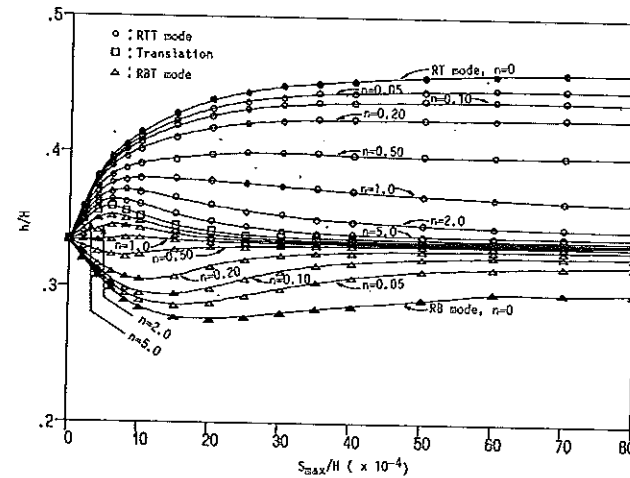


Fig. 13 Relative Height of Resultant Pressure Application versus Wall Movement

move. The gradual release of the concentrated stress near the base with further wall movement raises the point of application of the total thrust to a limiting value of $(h/H)_A = 0.30$. A similar trend of h/H variation can be observed from the experimental results plotted in Fig. 12, although the $(h/H)_A$ determined from the model test is only 0.28. With the increase of n value, analytical results tend to converge to that for translational mode. When an active state is reached, the analytical h/H value is found to be 0.34 for T mode. As indicated in Fig. 3, the experimental high stress near the top and the low stress measured near the base cause the point of application of $P_{A,h}$ to act at 0.40 H from the base of the wall.

Under RT mode, due to the build up of arching stress near the top of the wall and the relaxation of earth pressure near the base (see Fig. 7), the point of application of P_h moves up with increasing wall movement. When an active state is reached, the h/H value is found to be 0.46 as indicated in Fig. 13. The $(h/H)_A$ obtained is in good agreement with the model test result. It is evident from Fig. 13 that with the increase of n value, the variation of h/H tends to converge with the pattern induced by the translational mode. It is clear from Fig. 13 and Fig. 12 that the RB, RT and T modes are actually the three limiting wall movements that could occur to a rigid wall.

CONCLUSIONS

The finite element method has been used to study the influence of wall movement on the variation of earth pressure. Lateral stresses induced by the RBT and RTT wall movements have been investigated. Based on the analytical results obtained from this study, the following conclusions can be drawn.

1. For a wall under translational movement, the intensity and distribution of active earth pressure are in good agreement with the values calculated following the Coulomb's theory.
2. For a wall under RBT mode, unless the n value is less than 0.50, the induced active earth pressure distribution can be adequately estimated using the Coulomb's theory. Stress concentration that acts near the base of the wall plays an important role for n values less than 0.50.
3. For a wall under RTT mode, the arching stress acts at upper elevations of the wall for low n values. However, the active earth pressure distribution can be properly predicted by the Coulomb's theory for n values greater than 2.0.
4. For both RBT and RTT modes, the magnitude of the active total thrust decreases with increasing n value. The translational mode constitutes the lower bound for both RBT and RTT types of wall movements.
5. With the increase of n value, the point of application of the total thrust tends to converge with that induced by the translational mode. The RB, RT and T modes are actually the three limiting wall movements that could occur to a rigid wall.
7. The mode of wall movement has a significant effect on the generation of earth pressure.

ACKNOWLEDGEMENTS

The writers wish to acknowledge the financial assistance of the National Science Council of the ROC government (NSC77-0410-E009-06) which made this investigation possible. The writers are grateful to Dr. Isao Ishibashi, Old Dominion Univ., for his initial guidance of the subject. The writers are also grateful to Dr. James M. Duncan, Virginia Tech., who provided detailed information concerning the hyperbolic stress-strain model. Spicial thanks are due to Dr. Yii-Wen Pan, Mr. Yuh-Jiun Huang, and Mr. Chung-Yih Chang, National Chiao Tung Univ., for their valuable input.

REFERENCES

- CLOUGH, G.W. and DUNCAN, J.M. (1971). Finite element analysis of retaining wall behavior. *Journal of Soil Mechanics and Foundation Engineering Division, ASCE*, Vol. 97, No. SM12, pp. 1657-1673.
- DUNCAN, J.M. (1980). Hyperbolic stress-strain relationships. *Proceedings, Limit Equilibrium, Plasticity and Generalized Stress-strain in Geotechnical Engineering*, McGill University, May 28-30, pp 443-460.
- DUNCAN J.M. and CHANG, C.Y. (1970). Nonlinear analysis of stress and strain in soils. *Journal of Soil Mechanics and Foundation Engineering Division, ASCE*, Vol. 96, No. SM5, pp. 1625-1653.
- DUNCAN, J.M. and SEED, R.B. (1986). Compaction-induced earth pressures under K_0 -conditions. *Journal of Geotechnical Engineering, ASCE*, Vol. 112, No. 1, pp. 1-12.
- DUNCAN, J.M., BYRNE, P., WONG, K.S. and MABRY, P. (1980). Strength, stress-strain and bulk modulus parameters for finite element analyses of stresses and movements in soil masses. *Geotechnical Engineering Report, UCB/GT/80-01*, University of California, Berkeley, California.
- FANG, Y.S. (1983). Dynamic earth pressures against rotating walls. Dissertation submitted for the degree of Doctor of Philosophy, University of Washington, Seattle, Washington.
- FANG, Y.S. and ISHIBASHI, I. (1986). Static earth pressures with various wall movements. *Journal of Geotechnical Engineering, ASCE*, Vol. 112, No. 3, pp. 317-333.
- GOODMAN, R.E., TAYLOR, R.L. and BREKKE, T.L. (1968). A model for the mechanics of jointed rock. *Journal of Soil Mechanics and Foundations Division, ASCE*, Vol. 94, No. 3, pp. 637-659.
- JANBU, N. (1963). Soil compressibility as determined by oedometer test and triaxial tests. *Proceedings, European Conference on Soil Mechanics and Foundation Engineering*, Vol. 1, Weisbaden, Germany, pp. 19-26.
- KONDNER, R.L. (1963). Hyperbolic stress-strain response: cohesive soils. *Journal of the Soil Mechanics and Foundations Division, ASCE*, Vol. 89, No. SM1, pp. 115-143.

- NAKAI, T. (1985). Finite element computations for active and passive earth pressure problems of retaining wall. *Soils and Foundations, JSSMFE, Vol. 25, No. 3*, pp. 98-112.
- POTTS, D.M. and FOURIE, A.B. (1986). A numerical study of the effects of wall deformation on earth pressures. *International Journal of Numerical and Analytical Methods in Geomechanics, Vol. 10*, pp. 383-405.
- POTYONDY, J.G. (1961). Skin Friction between various soils and construction materials. *Geotechnique, Vol. 11, No. 4*, pp. 339-353.
- SHERIF, M.A., FANG, Y.S. and SHERIF, R.I. (1984). K_a and K_o behind rotating and non-yielding walls. *Journal of Geotechnical Engineering, ASCE, Vol. 110, No. 1*, pp. 41-56.
- SHERIF, M.A., ISHIBASHI, I. and LEE, C.D. (1982). Earth pressure against rigid retaining wall. *Journal of Geotechnical Engineering, ASCE, Vol. 108, No. 5*, pp. 679-695.
- SIMPSON, B. and WROTH, C.P. (1972). Finite elements for a model retaining wall in sand. *Proceedings, 5th European Conference of Soil Mechanics and Foundation Engineering, Madrid, Spain*, pp. 85-94.
- TERZAGHI, K. (1934). Large retaining wall test. *Engineering News Record, Vol. 112*, pp. 136-140.
- TERZAGHI, K. (1943). *Theoretical Soil Mechanics*. John Wiley and Sons, Inc., New York, N.Y., pp. 67.

APPENDIX I. NOTATION

The following symbols are used in this paper:

- B = bulk modulus
 c = cohesion of soil
 D_r = relative density of soil
 $D_{10}, D_{30}, D_{50}, D_{60}$ = soil diameters of which 10, 30, 50, and 60%, respectively, by weight is finer than
 E = Young's modulus
 E_i = Initial tangent modulus
 E_t = tangent modulus
 e_{max}, e_{min} = Maximum and minimum void ratio of soil
 G_s = specific gravity
 h = distance between the point of application of the resultant force and the wall base
 H = height of backfill from the wall base
 K = modulus number for primary loading
 $K_{A,h}$ = coefficient of active horizontal soil thrust
 K_b = bulk modulus number

EARTH PRESSURES UNDER WALL

- K_h = coefficient of horizontal soil thrust
 K_l = stiffness number
 K_n = normal stiffness
 K_o = coefficient of earth pressure at-rest
 K_s = shear stiffness
 K_{si} = initial stiffness modulus at interface
 K_{st} = tangent stiffness number
 m = bulk modulus exponent
 η = parameter indicating location of the center of rotation of wall
 n_1, n_2 = modulus exponents
 P = resultant of earth pressure
 P_a = atmospheric pressure
 $P_{A,h}$ = resultant of horizontal active earth pressure
 P_h = resultant of horizontal earth pressure
 P_v = resultant of vertical earth pressure
 R_f = failure ratio
 s_{max} = maximum wall displacement
 z = depth from the top of backfill
 γ = unit weight
 δ = wall friction angle
 Δ_n = interface normal displacement
 Δ_s = interface shear displacement
 ϵ = normal strain
 $\Delta\epsilon_x, \Delta\epsilon_y, \Delta\gamma_{xy}$ = strain increments
 σ_1 = major principal stress
 σ_3 = minor principal stress
 σ_h, σ'_h = horizontal earth pressure
 σ_n = normal stress
 σ_v, σ'_v = vertical earth pressure
 $(\sigma_1 - \sigma_3)_f$ = stress difference at failure
 $\Delta\sigma_x, \Delta\sigma_y, \Delta\tau_{xy}$ = stress increments
 τ = shear stress
 τ_f = shear stress at failure
 ϕ = internal friction angle